Dam-break flows of water-granular mixtures: A numerical study

Nuttita Pophet, Research Assistant, NCCHE, Oxford, MS, nuttita@ncche.olemiss.edu
Mustafa Altinakar, Director and Research Professor, NCCHE, Oxford, MS, altinakar@ncche.olemiss.edu
Yavuz Ozeren, Research Assistant Professor, NCCHE, Oxford, MS, yozeren@ncche.olemiss.edu

Abstract

Dam-break flows of water-granular mixtures such as landslides, debris flows and tailings-dam break flows, are often catastrophic events. These types of flows can cause loss of life, property damage and environmental problems. Understanding the dynamic behavior of these types of flows and developing reliable predictive mathematical and numerical models for solving real-life problems are therefore necessary. In this study, dam-break flows of water-granular mixtures are investigated numerically by taking into account the presence of porous flow in the deforming granular mass. The numerical model is solved by coupling two solvers in the open source finite-volume platform OpenFOAM. The *interFoam* solver simulates the movement of a water-granular mixture by solving the Navier-Stokes equations. The free surface is captured using the volume of fluid (VOF) method. Shear stresses due to inter-particle contacts in the mixture are modeled by making use of a pressure-dependent, effective shear viscosity. This effective viscosity is calculated by using the instantaneous pore water pressure field provided by the *porousInterFoam* solver. The *porousInterFoam* solver is a modified version of *interFoam* to simulate porous flow in the granular matrix by including a sink term in the momentum equation to account for the pressure drop when porous medium is present in the domain. The coupled model is validated against laboratory experiments of dam-break flows of water-granular mixtures conducted in the dam-break facility of NCCHE at the USDA-ARS National Sedimentation Laboratory in Oxford, Mississippi.

Introduction

Granular flows, driven by gravity force, are mass movements of mixtures of solid particles and interstitial fluid. Examples include landslides, debris flows, and tailings dam-break flows, for which the interstitial fluids are water and/or air. These types of flows can be extremely destructive for human lives, properties and infrastructure, and the environment. Understanding the dynamic behavior of these types of flows and developing reliable predictive models are important. The development of numerical models for granular flows centers around three main issues: choice of a level of approximation of the flow field and pressure field in the model, choice of coupling between the solid and fluid phases, and choice of a rheological model or a constitutive equation. Granular flows have been extensively studied using numerical models based on depth-averaged shallow water equations. The experimental data suggests that replacement of the vertical distribution of velocity by a depth-averaged velocity and the omission of vertical velocities does not reflect true flow behavior and may lead to incorrect predictions in the region of strong vertical velocity gradient. Moreover, because such models ignore the velocity component normal to the bed, they account for solid-solid and solid-fluid interaction effects only in a rudimentary way (Iverson, 1997).

Based on the level of coupling between solid and fluid phases, theoretical models can be categorized into: single-phase flow, and two-phase mixture models. Single-phase flow models treat the mixture as a homogeneous material and employ a non-Newtonian rheological model to incorporate the effect of grain-grain interaction (Berzi et al., 2010). The rheologies adopted range from visco-plastic (Bingham, 1922) to collisional regime (Bagnold, 1954). However, as emphasized by Meng and Wang (2016), although such simple models can describe the dynamic behavior of the mixture to some extent, they are unable to account for complex interactive coupling between the fluid and granular phases or the dynamic behavior of each phase.

The two-phase mixture models can be classified as two-phase and mixture models. In the two-phase model, the momentum and continuity equations of each phase are solved separately (e.g., Armanini, 2013). Coupling is achieved through the pressure and inter-phase exchange coefficients. When there is a wide distribution of the particulate phase or when the interphase laws are unknown or their reliability becomes questionable, however, the mixture model is a good substitute for the two-phase approach in many cases (Ansys Fluent, 2009). In the mixture model, the continuity and momentum equations for the mixture are solved together with algebraic expressions for the relative velocities (Savage et al., 2014). This model can be used to simulate grain-fluid flows where the phases move at different velocities, but assume a local equilibrium over short spatial length scale. In this way, the model can incorporate a separate response from the interstitial fluid and the solid phase.

Choice of a constitutive equation is an important consideration when modeling granular flows. Unlike Newtonian fluids, which are well described by the Navier-Stokes equations, no constitutive law can reproduce the diversity of behavior observed with a cohesionless granular material (Forterre and Pouliquen, 2008). This difficulty originates from fundamental characteristics of granular matter such as negligible thermal fluctuation, highly dissipative interactions, and a lack of separation between the microscopic grain scale and the macroscopic scale of the flow (Goldhirsch, 2003). As a result, granular flows are often divided into three regimes and the appropriate constitutive equation is chosen based on the flow regime. In a quasi-static regime, the deformations are very slow and the particles interact by frictional contacts. The most frequently adopted constitutive relation for the quasi-static regime is the shear rate-independent models based on Mohr-Coulomb (M-C) theory. A grain-inertia regime is the regime where the flow is very rapid and dilute, and the particles interact by collisions. The shear rate-dependent relationships are mostly based on extension of the kinetic theory. In an intermediate regime, the material is dense but still flows like a liquid, with the particles interacting with each other both by collision and friction. The so-called μ(I)-rheology has been developed for this regime (GDR MiDi, 2004).

In this study, a 3-D numerical model for mixture flows is developed by coupling the model of grain-fluid mixture flow with the model of flow in porous media. The coupled model is built on the open-source finite-volume platform OpenFOAM, which provides a library of numerical schemes necessary for the discretizations. The *interFoam* and *porousInterFoam* solvers with some modifications are employed for flows of mixture and flows in porous media, respectively. To investigate the efficiency and accuracy of the coupling technique, the developed model is verified by experimental data of granular dam-break flows.

Materials and Methods

Governing Equations

Mixture Flows (*interFoam*)**:** Granular/debris flows are usually treated as a motion of continuum despite the fact that they contain solid particles. This approximation makes the

equations of mass and momentum conservation for granular flows similar to those for the motion of a generic fluid (Lorenzini and Mazza, 2004). The governing equations can be written in the differential form as:

$$\nabla \cdot \boldsymbol{u} = 0 \tag{1}$$

$$\frac{\partial \rho_m \boldsymbol{u}}{\partial t} + \nabla \cdot (\rho_m \boldsymbol{u}\boldsymbol{u}) = \rho_m \boldsymbol{g} + \nabla \cdot \boldsymbol{\sigma} \tag{2}$$

where:

$\boldsymbol{u}$ is the velocity vector;

$\boldsymbol{g}$ is the gravitational acceleration vector;

ρ_m is the density of the mixture with $\rho_m = (1-n)\rho_s + n\rho_f$, where n is the porosity, and ρ_s and ρ_f are the density of the solid particles and the interstitial fluid, respectively;

$\boldsymbol{\sigma}$ is the stress tensor, generally expressed as $\boldsymbol{\sigma} = -p\mathbf{I} + \boldsymbol{\tau}$; where p is pressure, $\mathbf{I}$ is the unit tensor and $\boldsymbol{\tau}$ is the shear stress tensor,

$$\boldsymbol{\tau} = 2\mu_{eff}(\|\boldsymbol{D}\|, p)\boldsymbol{D} \tag{3}$$

where $\boldsymbol{D} = \boldsymbol{D}(\boldsymbol{u}) = (\nabla \boldsymbol{u} + (\nabla \boldsymbol{u})^{\boldsymbol{T}})/\mathbf{2}$ is the strain rate tensor, and $\|\boldsymbol{D}\|$ is second invariant of the strain rate tensor: $\|\boldsymbol{D}\| = \sqrt{2\boldsymbol{D}_{ij}\boldsymbol{D}_{ij}}$. In the case of a dry granular flow, an interstitial fluid plays no significant role in the dynamics of the flow. The effective viscosity can be defined as

$$\mu_{eff} = (\|\boldsymbol{D}\|, p) = \frac{\mu p}{\|\boldsymbol{D}\|} \tag{4}$$

where μ is analogous to a coefficient of friction. Within this description, the granular mixture is then described as an incompressible non-Newtonian fluid, with an effective viscosity (μ_{eff}) depending on both the shear rate and the pressure, a signature of the underlying frictional nature of the medium (Forterre and Pouliquen, 2008). This description is similar to the one developed in other viscoplastic materials like mud. A flow threshold is given by a frictional Drucker-Prager criterion (Drucker and Prager, 1952) for which $|\boldsymbol{\tau}| > \mu p$ is recovered when $\|\boldsymbol{D}\|$ goes to zero and the viscosity diverges as can be seen in Eq. (3) and (4).

In the case of an initially saturated grain-fluid mixture, the total mixture pressure (p) is replaced by the effective inter-particle normal stress (p_{eff}) which is approximated by subtracting the pore water pressure (p_f) from the total mixture pressure. This definition of effective stress correspond to Terzeghi's effective stress. The effective viscosity can be defined as:

$$\mu_{eff}\left(\|\boldsymbol{D}\|, p_{eff}\right) = \frac{\mu(p - p_f)}{\|\boldsymbol{D}\|} + k(\|\boldsymbol{D}\|)^{n-1} \tag{5}$$

where k is the consistency index and n is the flow index. The effective viscosity is then the sum of a frictional term and a viscous term. The consistency index (k) and the flow index (n) are model calibration parameters. In this study, $k = 0.3$ and $n = 0.33$ give the most promising results. The pore water pressure (p_f) is obtained by solving porous media flows through the mixture as described in detail in the next subsection.

Porous Media Flows (*porousInterFoam*)**:** In this study, the macroscopic governing equations for the fluid flow in porous media derived by Wang et al., 2015 are employed. The macroscopic equations is obtained by the technique of volume averaging of the microscopic continuity and momentum equations over a representative elementary volume (REV). The intrinsic phase average is used in the derivation and defined by

$$\langle \varphi_f \rangle^f = \frac{1}{V_f} \int_{V_v} \varphi_v dV \tag{6}$$

where the subscript f means fluid quantity which refers to the portion of fluid existing within the gaps of the solid skeleton, V_f represents the volume of the fluid phase within the representative elementary volume V, and φ_f is a quantity associated with the fluid phase. The intrinsic phase average can be related to the phase average (also called Darcy's quantities) with $\langle \varphi_f \rangle = n \langle \varphi_f \rangle^f$, where n is the porosity. As concluded by Wang et al., 2015, the macroscopic conservation equations derived using the intrinsic phase average velocity are Galilean invariant. The following macroscopic equations can be obtained

$$\nabla \cdot \boldsymbol{u_f} = 0 \tag{7}$$

$$\frac{\partial \rho_f \boldsymbol{u_f}}{\partial t} + \nabla \cdot \left(\rho_f \boldsymbol{u_f} \boldsymbol{u_f} \right) = -\nabla p_f + \mu_f \nabla \cdot \left[\nabla \boldsymbol{u_f} + (\nabla \boldsymbol{u_f})^T \right] + \boldsymbol{F} \tag{8}$$

where ρ_f is the fluid density, $\boldsymbol{u_f}$ is the intrinsic phase average velocity, p_f is the pore pressure, μ_f is the fluid dynamic viscosity and $\boldsymbol{F}$ is the total body force including the resistance from the porous medium and other external forces and defined by

$$\boldsymbol{F} = -\frac{\mu_f n}{K} \left(\boldsymbol{u_f} - \boldsymbol{u_p} \right) - \rho_f \frac{n^2 F_n}{\sqrt{K}} \left(\boldsymbol{u_f} - \boldsymbol{u_p} \right) \left| \boldsymbol{u_f} - \boldsymbol{u_p} \right| + \rho_f \boldsymbol{g} \tag{9}$$

where K is the permeability, $\boldsymbol{g}$ is the gravitational acceleration, $F_n = 1.75/\sqrt{150 n^3}$ is the geometric function of the porous medium, and $\boldsymbol{u_p}$ is the velocity of the moving porous medium. In the case as $n = 1$ (i.e., in the absence of porous media) the value of K will become infinite, and the above equations reduces to the Navier-Stokes equations for pure fluid flows. By modeling porous media flows in this way, the flows inside and outside the porous medium are solved with the same set of equations. This approach avoids the need to specify matching conditions at the pure fluid and porous medium interface, at which interface jump conditions were defined for velocity and shear stresses (del Jesus et al., 2012). Further details of the derivation can be found in Wang et al., 2015.

The Coupling Algorithm

In order to couple *interFoam* and *porousInterFoam*, a python library is developed to wrap the two solvers into a main program. A flowchart of the coupled algorithm is presented in Figure 1. In the flowchart, after the main program starts, geometry, parameters, constants and coefficients are initialized. At half time step of the mixture solver (*interFoam*), the porous flow model (*porousInterFoam*) is solved. At this stage, pore water pressure (p_f) is obtained and sent to the mixture model to calculated the viscous shear stress. Then, the mixture model is solved for grain-

fluid mixture flow. At this stage, geometry of the porous medium and mixture velocity are obtained and sent back to the porous flow model. These steps continue until the simulation ends.

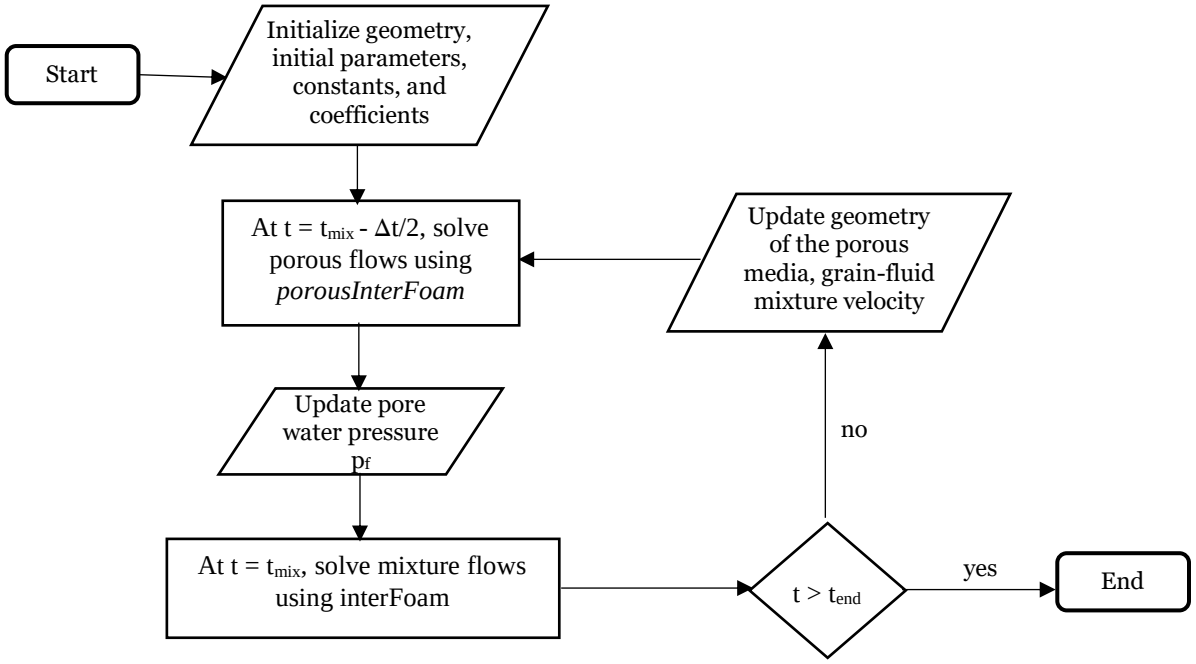

Figure 1. Detailed relationship of *porousMixtureInterFoam* algorithm.

Experimental Setup

Figure 2. PET pellets.

An experiment (Rebillout et al., 2017) conducted in the dam-break facility of National Center for Computational Hydroscience and Engineering (NCCHE) at the USDA-ARS National Sedimentation Laboratory in Oxford, Mississippi is used to validate the coupled model. In this experiment, the channel with a 7.6 m long flume having a width of 0.5 m and a height of 0.6 m was divided by a sliding gate into: (i) a 3.24 m length of upstream reservoir, and (ii) a 4.36 m length of dam-break channel. The PET pellets used in the experiment and the experimental setup are shown in Figure 2 and Figure 3. Some of the intrinsic and bulk properties of the material are summarized in Table 1. In the table, D_m is the mean nominal diameter, *Sf* is the shape factor, *n* is the porosity, ρ_{PET} is the density of the PET pellets, *K* the (packed) hydraulic conductivity, and ϕ is the friction angle. At the beginning of the experiments, the sliding gate is pulled upward with a speed of about 8 m/s to release the mixture of PET pellets and water to the downstream channel. Blue dye was added to the water in order to facilitate the tracking of the phreatic surface by imaging techniques. The flow fields in the upstream reservoir and the downstream channel were recorded using two and four high-speed cameras, respectively.

Table 1. Properties of the PET pellets (Ozeren et al., 2014).

d_{10} (mm)	d_{50} (mm)	d_{90}(mm)	D_m (mm)	*Sf*	*n* (packed)	ρ_{PET} (kg/m^3)	*K* (mm/s)	ϕ (°)
2.812	2.867	2.920	2.861	0.832	0.34	1422	16.6	30

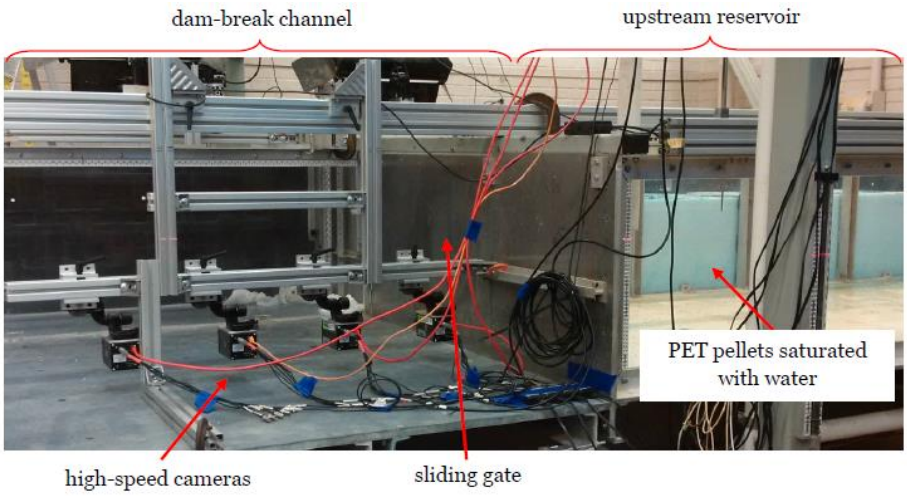

Figure 3. Experimental setup (Rebillout et al., 2017).

Simulation Setup

In the numerical simulation, the 3.93 m-long and 0.5 m-high computational domain (Figure 4) is initialized as two zones with different initial properties: (i) the mixture zone containing PET pellets saturated with water, and (ii) the empty cell zone. This domain is used for both the *interFoam* solver for mixture flow and the *porousInterFoam* solver for flow in porous media. In the mixture flow model, the wall boundary condition is used for the left boundary while atmosphere and open boundary conditions are used for the top and right boundaries, respectively. At the bottom, the Coulomb slip boundary condition is employed. For the porous flow model, boundary conditions are the same as the mixture model except at the bottom where the slip boundary condition is used. For both solvers, the time step is set to 0.001 s while the cell size is 0.01 m.

Simulation Results

Mixture Profiles and Velocity Fields

Figure 5 shows the mixture profiles of the simulation and the experiment and velocity magnitude for the simulation at time 0.25, 0.5, 1.25, 1.5, 2.0 and 2.25 s. At time t = 0.25 s, the mixture column starts falling and the front starts moving in both the simulation and the experiment. The maximum velocity is concentrated at the front of the mixture profile with the magnitude of about 0.5 m/s. At time t = 0.5 s, the velocity magnitude develops at the front to the maximum of about 0.75 m/s. The front in the simulation is almost at the same location as the experiment which is at about x = 0.24 m. However, there is discrepancy between the shapes of the mixture in the simulation and the experiment. This may be due to the expansion (change in porosity and volume fraction of grains) of the densely-packed grain column while shearing. Since the model does not consider this effect, no expansion is allowed in the simulation. However, even neglecting this effect, the model can still reproduce the experiment from the initial falling stage, the flowing stage to the stopping stage. The front in the simulation propagates at almost the same speed as the experiment. At time t = 2.25 s, the velocity magnitude of almost zero is observed in the simulation which indicates that the model can predict the stopping stage.

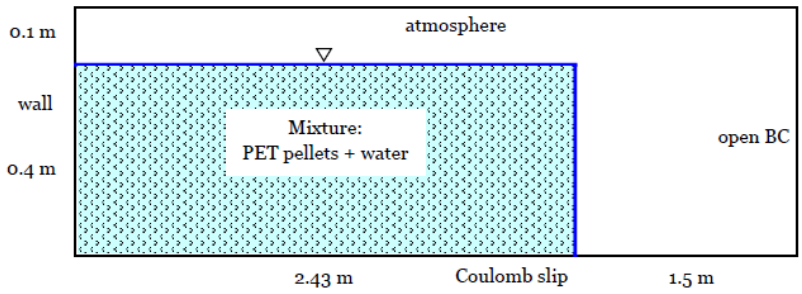

Figure 4. Computational domain.

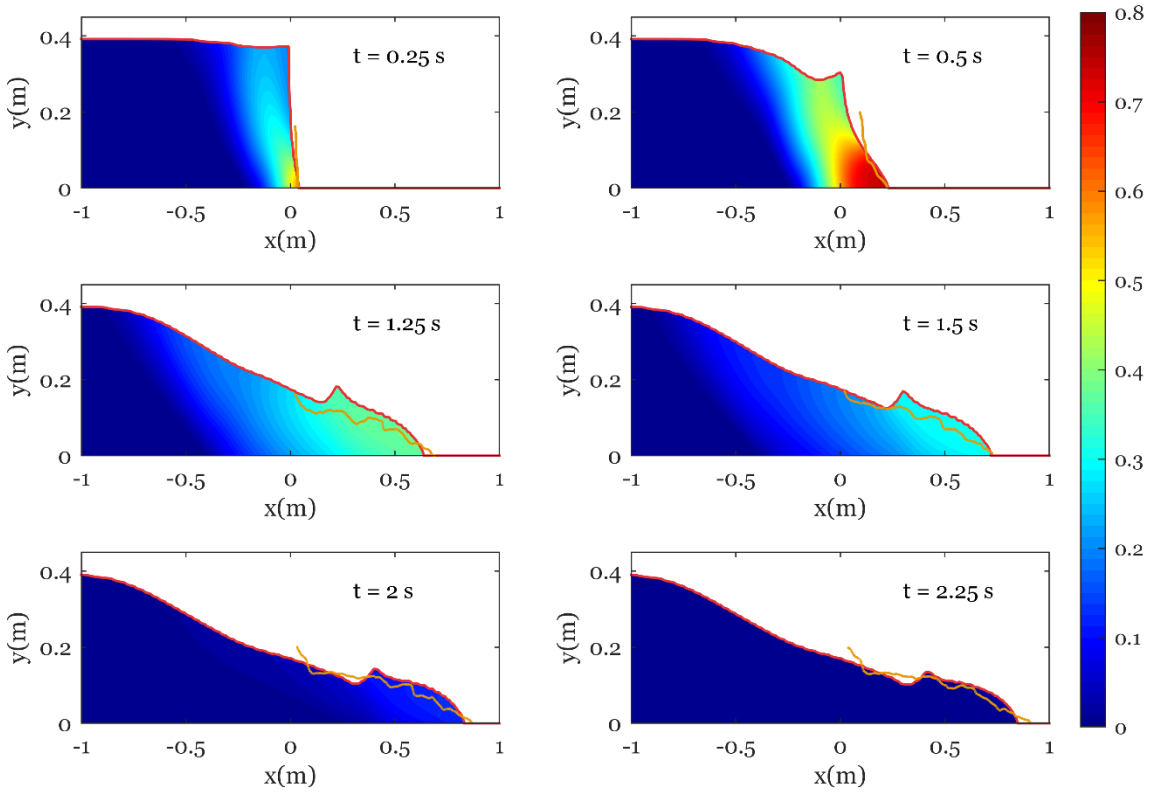

Figure 5. Comparison of the mixture profiles between the simulation (red line) and the experiment (yellow line), and velocity magnitude for the simulation at different times.

Pressure Distribution and Strain Rate

Figure 6 shows pressure distribution and shear rate of the mixture obtained from the simulation at time t = 0.25, 0.5 and 1.25 s. The figure shows that pressure varies from 0 at the interface to about 4000 Pa near the bed in the non-flowing region where the mixture velocity is almost zero (see Figure 5 for the velocity field). At time t = 0.25 s, the strain rate is concentrated near the bottom front of the mixture profile with the maximum of about 7 s^{-1} while at time t = 1.25 s the maximum of about 1.5 s^{-1} is observed near x = -0.4 m.

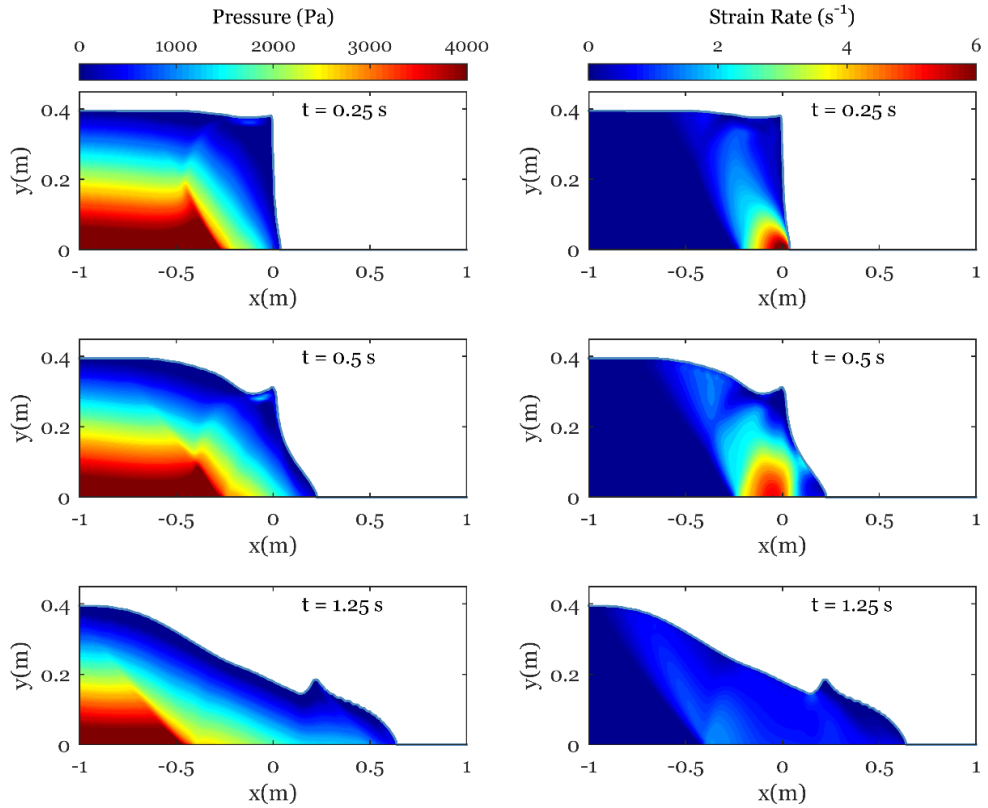

Figure 6. Pressure distribution and shear rate obtained from the simulation at different times.

Comparison of Simulated and Experimental Mixture Profiles

Figure 7 shows the mixture profiles obtained from the simulation and extracted from the experiment over a snapshot of the experiment at the final deposit (t = 2.25 s). It can be seen that the extracted profile (yellow line) follows the surface near the glass wall. However, the profile inside is different in some locations and the flow is not 2D. As a result, it is difficult to define the surface in the experiment. This may be one of the reasons for the difference between the profiles observed in Figure 5. The other issue is the front deposit. The mixture stops somewhat sooner in the simulation than in the experiment. This may be due to the bed friction coefficient used in the Coulomb slip boundary condition in which the value is set to the same value as an internal friction coefficient.

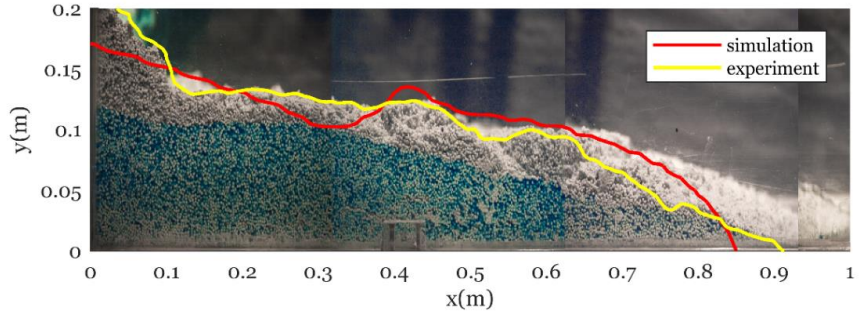

Figure 7. Plots of the mixture profiles obtained from the simulation (red) and extracted from the experiment (yellow) over a snapshot of the experiment at the final deposit (t = 2.25 s).

Conclusion

A numerical model is developed by coupling the mixture model with the porous model using OpenFOAM software. The two main solvers used are the *interFoam* for grain-fluid mixture flows and the *porousInterFoam* for flows in porous media. These two solvers solve the governing equation analogous to the Navier-Stokes equation but with additional terms or different physical interpretation of an existing term. The coupled model is validated using experimental data. The comparison shows good agreement between the simulated and measured granular profiles and the front evolution.

References

Ansys Fluent. 2009. Theory Guide. Ansys Inc 5.5.

Armanini, A. 2013. "Granular flows driven by gravity," Journal of Hydraulic Research, 51(2):111–120.

Bagnold, R.A. 1954. "Experiments on a gravity-free dispersion of large solid spheres in a Newtonian fluid under shear," Proceedings of the Royal Society of London. Series A, 225(1160):49–63.

Berzi, D., Jenkins, J.T., and Larcher, M. 2010. "Debris flows: Recent advances in experiments and modeling," Advances in Geophysics, 52:103–138.

Bingham, E.C. 1922. Fluidity and plastic (Vol. 2). McGraw-Hill.

Del Jesus, M., Lara, J.L., and Losada, I.J. 2012. "Three-dimensional interaction of waves and porous coastal structures: Part I: Numerical model formulation," Coastal Engineering, 64:57–72.

Drucker, D.C., and Prager, W. 1952. "Soil mechanics and plastic analysis or limit design," Quarterly of Applied Mathematics, 10(2):157–165.

Forterre, Y., and Pouliquen, O. 2008. "Flows of dense granular media," Annual Review of Fluid Mechanics, 40:1–24.

GDR MiDi. 2004. "On dense granular flows," The European Physical Journal, 14(4):341–365.

Goldhirsch, I. 2003. "Rapid granular flows," Annual Review of Fluid Mechanics, 35(1):267–293.

Iverson, R.M. 1997. "The physics of debris flows," Review of Geophysics, 35(3):245–296.

Lorenzini, G., and Mazza, N. 2004. Debris flow: Phenomenology and rheological modeling. Wit Press, Boston.

Meng, X., and Wang, Y. 2016. "Modelling and numerical simulation of two-phase debris flows," Acta Geotechnica, 11(5):1027–1045.

Ozeren, Y., Aleixo, R., Marsooli, R., and Altinakar, M. 2014. Physical properties of artificial sediment.

Rebillout, L., Ozeren, Y., and Altinakar, M. 2017. Dam break experiments with granular material.

Savage, S.B., Babael, M.H., and Dabros, T. 2014. "Modeling gravitational collapse of rectangular granular piles in air and water," Mechanics Research Communications, 56:1–10.

Wang, L., Wang, L.P., Guo, Z., and Mi, J. 2015. "Volume-averaged macroscopic equation for fluid flow in moving porous media," International Journal of Heat and Mass Transfer, 82:357–368.